Neuroanatomical and Functional Consequences of Oxytocin Treatment at Birth

William M. Kenkel, Richard J. Ortiz, Jason R. Yee, Allison M. Perkeybile, Praveen Kulkarni, C. Sue Carter, Craig F. Ferris

ABSTRACT:

Birth is a critical period for the developing brain, a time when surging hormone levels help prepare the fetal brain for the tremendous physiological changes it must accomplish upon entry into the 'extrauterine world'. A number of obstetrical conditions warrant manipulations of these hormones at the time of birth, but we know little of their possible consequences on the developing brain. One of the most notable birth signaling hormones is oxytocin, which is administered to roughly 50% of laboring women in the United States prior to / during delivery. Previously, we found evidence for behavioral, epigenetic, and neuroendocrine consequences in adult prairie vole offspring following maternal oxytocin treatment immediately prior to birth. Here, we examined the neurodevelopmental consequences in adult prairie vole offspring following maternal oxytocin treatment immediately. Control prairie voles and those exposed to 0.25 mg/kg oxytocin were scanned as adults using anatomical and functional MRI, with neuroanatomy and brain function analyzed as voxel-based morphometry and resting state functional connectivity, respectively. Overall, anatomical differences brought on by oxytocin treatment, while widespread, were generally small, while differences in functional connectivity, particularly among oxytocin-exposed males, were larger. Analyses of functional connectivity based in graph theory revealed that oxytocin-exposed males in particular showed markedly increased connectivity throughout the brain and across several parameters, including closeness and degree. These results are interpreted in the context of the organizational effects of oxytocin exposure in early life and these findings add to a growing literature on how the perinatal brain is sensitive to hormonal manipulations at birth.

BACKGROUND:

Oxytocin (OXT) is a potent and pleiotropic hormone that surges at birth to help facilitate the tremendous changes that both mammalian mothers and their offspring must accomplish upon delivery [1,2]. As of 2019, 29.4% of laboring women in the U.S. received OXT to induce labor [3], and according to available survey data, this figure raises to ~50% of birthing women in America when considering OXT used to either induce and/or augment labor [4]. This obstetric practice is of interest to neuroscience because there is evidence OXT can cross the placenta [5] and a growing literature suggests the neonatal brain is particularly sensitive to OXT around the time of birth, when OXT receptor (*Oxtr*) expression begins to accelerate [6] and OXT neurons in the brain undergo intense remodeling [7]. Indeed, the long-term, developmental effects of OXT manipulations in early life are well-documented [8,9], which suggests the perinatal period may be a *sensitive period* with regard to the impact of OXT.

Some initial studies suggested higher rates of autism spectrum and attention deficit / hyperactivity disorder amongst children born to women whose labors were induced with OXT; however, meta-analysis of such findings suggest that any such conclusions remain premature [10]. While there have been conflicting reports as to whether OXT administered to induce / augment labor is associated with increased rates of autism spectrum disorder or autistic-like behavior in offspring, considerations of dose add an important degree of nuance to this topic [11,12]. Thus, regardless of whether the consequences of obstetrically administered OXT raise to the level of a neurodevelopmental disorder, the question of whether OXT affects offspring neurodevelopment is of great public health relevance given its widespread use.

Previously, we investigated the impact of maternally administered OXT on offspring neurodevelopment and behavior using the socially monogamous prairie vole [13]. We found that fetal physiology was indeed sensitive to maternally administered OXT and that, in the fetal brain, such OXT dose-dependently increased methylation of the *Oxtr* promoter. In adulthood, OXT-exposed offspring of both sexes were found to demonstrate a broadly gregarious phenotype such that they exhibited more spontaneous alloparental care toward unrelated pups and spent more time in close social contact with opposite-sex adults. Male voles exposed to OXT also showed increased density of OXT receptor in the central amygdala, insular cortex, and parietal cortex, while showing decreased vasopressin receptor density in the ventral pallidum.

Because OXT is a pleiotropic hormone, we opted for a broad survey of the brain in the present study, carrying out whole-brain resting functional connectivity to further characterize the scope of the neurodevelopmental consequences of OXT exposure at birth. Here, we scanned adult prairie vole offspring of pregnant females treated with 0.25 mg/kg OXT on the expected day of delivery.

METHODS:

Subjects

Prairie vole offspring (*Microtus ochrogaster*) were generated as previously described [13]. All procedures were conducted in accordance with the National Institutes of Health Guide for the Care and Use of Laboratory Animals and were approved by the Institutional Animal Care and Use Committee of Northeastern University. On the expected day of delivery, pregnant females were either injected intraperitoneally with OXT (0.25 mg/kg, 'OXT') or left undisturbed ('Control'). Offspring were only included if they were delivered within 24 hours of OXT treatment. Offspring were raised by their birth parents as we previously observed no effect of maternal-OXT treatment on offspring outcomes [13]. At 20 days of age, OXT and Control offspring were weaned into same-sex sibling pairs and were left to mature. Upon reaching adulthood (postnatal days 60-70), OXT and Control offspring underwent three neuroimaging scans: aT1-weighted anatomical scan for voxel based morphometry scan (VBM), an awake, resting state functional scan (rs-fMRI), and an anesthetized diffusion-weighted imaging scan (DWI), as detailed below. Subject offspring consisted of 17 Control females, 19 Control males, 17 OXT females, and 16 OXT males. From these, 7 Control females, 12 Control males, 13 OXT females and 13 OXT males were ultimately included in the rs-fMRI analyses after removing subjects due to motion artefact or technical difficulties.

Neuroimaging

All neuroimaging measures were collected using a Bruker BioSpec 7.0T/20-cm Ultra Shield Refrigerated horizontal magnet (Bruker, Billerica, MA). A 20-G/cm magnetic field gradient insert (inner diameter 12 cm) was used to scan anesthetized subjects using a quadrature transmit/receive volume coil (inner diameter 38 mm). Imaging sessions began with an anatomical scan with the following parameters: 20 slices; slice thickness, 0.70 mm; field of view, 2.5 cm; data matrix, 256 x 3 x 256; repetition time, 2.5 seconds; echo time (TE), 12.0 ms; effective TE, 48 ms; number of excitations, 2; and total acquisition time, 80 seconds.

Voxel Based Morphometry (VBM)

The following procedures were adapted for use in the vole from those described previously for rats [14]. For each subject, the atlas (image size 256 x 256 x 63) (H × W × D) was warped from the standard space into the subject image space (image size 256 × 256 × 40) using the nearest-neighbor interpolation method. In the volumetric analysis, each brain region was therefore segmented, and the volume values were extracted for all 111 regions of interest (ROIs), calculated by multiplying unit volume of voxel (in mm^3) by the number of voxels using an in-house MATLAB script. To account for different brain sizes, all ROI volumes were normalized by dividing each subject's ROI volume by their total brain volume.

Diffusion-weighted Imaging (DWI)

The following procedures were identical to those described previously [15,16]. Diffusion-weighted imaging (DWI) was acquired with a spin-echo echo-planar imaging (EPI) pulse sequence with the following parameters: repetition time/TE, 500/20 ms; 8 EPI segments; and 10 noncollinear gradient directions with a single b-value shell at 1000 seconds/mm^2 and 1 image with a b-value of 0 seconds/mm^2 (referred to as b0). Geometrical parameters were as follows: 48 coronal slices, each 0.313 mm thick (brain volume) and with in-plane resolution of 0.313 x 3 x 0.313 mm^2 (matrix size, 96 x 3 x 96; field of view, 30 mm^2). The imaging protocol was repeated 2 times for signal averaging. DWI acquisition took 35 to 70 minutes. DWI included diffusion-weighted three-dimensional EPI image analysis producing fractional anisotropy (FA) maps and apparent diffusion coefficient. DWI analysis was implemented with MATLAB (version 2017b) (The MathWorks, Inc., Natick, MA) and MedINRIA version 1.9.0 (http://www-sop.inria.fr/asclepios/software/MedINRIA/index.php) software.

Each brain volume was registered with the three-dimensional MRI Vole Brain Atlas template (Ekam Solutions LLC, Boston, MA) allowing voxel- and region-based statistics [17]. In-house MIVA software was used for image transformations and statistical analyses. For each vole, the b0 image was coregistered with the b0 template (using a 6-parameter rigid-body transformation). The coregistration parameters were then applied on the DWI indexed maps for each index of anisotropy. Normalization was performed on the maps providing the most detailed and accurate visualization of brain structures. Normalization parameters were then applied to all indexed maps and then smoothed with a 0.3-mm Gaussian kernel. To ensure that preprocessing did not significantly affect anisotropy values, the nearest neighbor option was used following registration and normalization.

Resting State Functional MRI (rs-fMRI)

We used the same equipment and scanning protocols as in our recent work; for complete details see [17–19]. Data were analyzed as 111 nodes corresponding to brain regions specified in a vole-specific atlas [17]. Pearson's correlation coefficients were computed per subject across all node pairs (6105), assessing temporal correlations between brain regions. Then, r-values' (-1 to 1) normality were improved using Fisher's Z-transform. For each group, 111×111 symmetric connectivity matrices were constructed, each entry representing the strength of edge. An |Z|=2.3 threshold was used to avoid spurious or weak node connections [20].

Network Analyses

Graph theory network analysis was generated using Gephi, an open-source network and visualization software [21]. For all groups, the absolute values of their respective symmetric connectivity matrices were imported as undirected networks and a threshold of |Z|=2.3 was applied to each node's edges to avoid spurious or weak node connections [22].

Betweenness Centrality

Betweenness centrality analyzes occurrences where a node lies in the path connecting other nodes [23]. Let $n_{i,j}^{k}$ be the number of pathways from *i* to *j* going through *k*. Using these measures of connection, the betweeness of vertex *k* is:

$$B_k = \sum_{ij} \frac{n_{ij}^{k}}{n_{ij}}.$$

Degree Centrality

Degree centrality indicates the number of associations of a specific node [24]. Non-weighted, binary degree is defined as:

$$C_D(j) = \sum_{j=1}^{n} A_{ij}$$

where *n* is the number of rows in the matrix in the adjacency matrix **A** and the elements of the matrix are given by A_{ij}, the number of edges between nodes *i* and *j*.

Closeness Centrality

Closeness centrality measures the average distance from a given starting node to all other nodes in the network [25]. Closeness is defined as:

$$C(x) = \frac{N-1}{\sum_{y} d(y,x)}$$

where *d(y,x)* is the distance between vertices *x* and *y* and *N* is the number of nodes in the graph.

Statistics

Normality tests of control females, control males, OXT females and OXT males were performed to examine if parametric or non-parametric assumptions were required for future analysis. Shapiro-Wilk's tests were performed to examine normality assumption for degree, closeness and betweeness centrality values. Regional p-values that were greater than 0.05 were assumed to be normal. A corresponding list of nodes that classified a region is detailed in table S___. After assumptions of normality were validated, one-way ANOVA tests were used to compare differences in degree, closeness and betweenness centralities between groups. When necessary, a nonparametric Kruskal-Wallis test was performed if there was evidence against normality assumption. Statistical differences between groups were determined using a Mann-Whitney U test (a = 5%). The following formula was used to account for false discovery from multiple comparisons:

$$P(i) \leq \frac{i}{V} \frac{q}{c(V)}$$

P(i) is the p value based on the t test analysis. Each of 111 regions of interest (ROIs) (i) within the brain containing V ROIs. For graph theory measures, statistical analyses were calculated using GraphPad Prism version 9.0.0 for MacOS (GraphPad Software, San Diego, California USA, www.graphpad.com).

RESULTS:

We observed a number of differences in VBM measures; however most were small to very small in effect size (Figures __). Within the Control group, there was only a single sex difference in regional volume. Within the OXT group, however, OXT females had larger volumes in 8 of 17 cortical regions and smaller volumes in 11 brainstem / cerebellar regions compared to OXT males (Table __). Similarly, Control males had larger volumes in 9 of 17 cortical regions and smaller volumes in 9 brainstem / cerebellar regions compared to OXT males (Table __). Comparing within females, OXT treatment at birth resulted in smaller volumes in 4 of 17 cortical regions. Control animals generally had larger amygdalar volumes than OXT animals (4 of 6 subregions in males; 2 of 6 in females). When morphometry data from all 111 brain regions were loaded into a PCA, the overall explanatory value of dimensions 1 and 2 was modest (29.4% and 15.9% respectively) and there were impacts of both sex and treatment on dimension 1, with male sex and OXT treatment leading to greater values (Figure __).

We observed a broad, albeit subtle pattern of effects in OXT-exposed males in DWI measures. In terms of FA, Control animals showed small but widespread sex differences, with females having greater FA than males across brain regions, a pattern not present in OXT animals due to increased FA among OXT-exposed males (Figure __, Table __). When FA data from all 111 brain regions were loaded into a PCA, there were no effects of either sex or treatment detected. In terms of ADC, Control males had greater ADC values than Control females across many brain regions (Table __) and greater ADC values than OXT males across many brain regions as well (Table __). While we observed widespread ADC differences between Control males and females, we observed no sex differences in ADC in the OXT-exposed condition. The PCA for ADC revealed a discrepancy between Control males and all other groups, with the latter having greater dimension 1 values. Thus, across the brain, OXT males' ADC values more closely resembled Control females and OXT females than they did Control males.

In the analyses of functional connectivity, OXT males stood out as having a widespread pattern of greater connectivity. Whereas Control females were found to have significant functional connectivity in 5% of all possible connections, OXT females had significant connectivity in 7.2% of connections. Whereas Control males had connectivity in 6.3% of connections, OXT males had significant connectivity in 12.5% of connections. While OXT females largely resembled Control females (Figure __), OXT males had more regions significantly functionally connected and stronger correlations in such regions (Figure __).

Similarly, when we examined the degree of connectivity, OXT males again showed a robust, widespread increase across the brain, with the exception of the prefrontal cortex, where the pattern was still present but did not rise to the level of statistical significance (Figure __).

DISCUSSION:

Here we describe how, in prairie voles, exposure to exogenous OXT at birth can impact neurodevelopment in ways that impact neural anatomy and functioning into adulthood. Overall, anatomical differences, while widespread, were generally small, while differences in functional connectivity, particularly among OXT-exposed males, were larger. Anatomically, OXT at birth led to a slight reduction in amygdalar volume and OXT males in particular had slightly smaller cortices and slightly larger brainstem / cerebellums (Figure __). OXT at birth led to males resembling females in terms of FA and ADC (Figures __ and __). However, functionally, OXT males showed marked differences from all other groups. OXT at birth led males to display robustly increased functional connectivity throughout the brain (Figure __). This was particularly the case across the cortex and in the hippocampus (Figure __). What does this notably broad increase in functional connectivity mean for the OXT males? We have at present only a few hints.

Interestingly, the robust and widespread changes in OXT males' neural physiology (i.e. functional connectivity) were greater than the changes observed in neuroanatomy (i.e. VBM and DWI). If OXT males are continuously experiencing high levels of communication between brain regions, we would expect that to eventually produce changes in anatomical connectedness. Either our anatomical measures of connectivity were insufficiently sensitive to detect these changes, or the relatively small changes in anatomy we did detect are sufficient to produce functional changes that are comparatively more robust. The functional connectivity

scans were undertaken with subjects lightly anesthetized, so it is unlikely that OXT males were responding differentially to the conditions of scanning. Furthermore, we have observed no evidence of stress reactivity being affected by perinatal OXT in our previous studies.

One pattern generally observed in the brains of humans with autism spectrum disorders is diminished long-distance functional connectivity and increased short-distance functional connectivity. We saw no such pattern in the OXT males of the present study. While some epidemiological studies have suggested a link between autism spectrum disorders and perinatal oxytocin exposure [10], residual confounding by either genetic or environmental vulnerabilities, could explain this apparent association. Indeed, our previous work, we observed a broadly gregarious phenotype in OXT-exposed voles [13]; if such results translated to humans, they would support the contention that underlying vulnerabilities bring on both a need for OXT in the mother and susceptibility to autism spectrum disorders in the child. While our previous work found behavioral differences in both males and females exposed to OXT, which is somewhat in contrast to the present study's findings, we also found males to be much more affected by perinatal OXT in terms of neuroanatomy, which was assessed as the density of OXT and AVP receptors. Numerous previous studies have found sex- , dose-, and region-dependent effects of early life oxytocin manipulation [8,26].

There have been very few studies on the impact of birth interventions and subsequent brain development. In the realm of neuroanatomy, Deoni and colleagues recently reported that CS results in smaller brain volumes in neonatal mouse pups [27]. However, no such findings have been observed in human children or infants [28]. In terms of VBM and functional connectivity, OXT led males toward a more masculinized phenotype. In terms of ADC and FA, however, OXT led males toward a more feminized phenotype. Further work is needed to reveal the meanings of these differences.
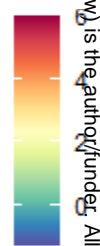
This study is not without limitations. Firstly, because the Control group did not receive a vehicle treatment, the effects of injection were not adequately controlled for, which introduced a stress confound of indeterminate magnitude. In a small validation study, adult offspring of saline-treated dams (n = 3 female, 5 male adult offspring) were not found to have meaningful differences in DWI values compared to the un-treated Control animals of the present study (n = 17 female, 19 male adult offspring).

REFERENCES:

1. Kenkel, W. M., Yee, J. R. & Carter, C. S. Is oxytocin a maternal-foetal signalling molecule at birth? Implications for development. *Journal of neuroendocrinology* **26,** 739–49 (2014).

2. Kingsbury, M. A. & Bilbo, S. D. The inflammatory event of birth: How oxytocin signaling may guide the development of the brain and gastrointestinal system. *Front.Neuroendocrinol.* **55,** 100794 (2019).

3. Martin, J. A., Hamilton, B. E., Osterman, M. J. K. & Driscoll, A. K. Births: Final Data for 2019. *Natl Vital Stat Rep* **70,** 1–51 (2021).

4. Declercq, E. R., Sakala, C., Corry, M. P., Applebaum, S. & Herrlich, A. Major Survey Findings of Listening to MothersSM III: Pregnancy and Birth. *J Perinat Educ* **23,** 9–16 (2014).

5. Malek, A., Blann, E. & Mattison, D. R. Human placental transport of oxytocin. *J.Matern.Fetal.* **5,** 245–255 (1996).

6. Rokicki, J. *et al.* Oxytocin receptor expression patterns in the human brain across development. (2021). doi:10.31219/osf.io/j3b5d

7. Madrigal, M. P. & Jurado, S. Specification of oxytocinergic and vasopressinergic circuits in the developing mouse brain. *Commun Biol* **4,** 1–16 (2021).

8. Hammock, E. A. D. Developmental Perspectives on Oxytocin and Vasopressin. *Neuropsychopharmacology* **40,** 24–42 (2015).

9. Bales, K. L. & Perkeybile, A. M. Developmental experiences and the oxytocin receptor system. *Horm.Behav.* **61,** 313–319 (2012).

10. Lønfeldt, N. N., Verhulst, F. C., Strandberg-Larsen, K., Plessen, K. J. & Lebowitz, E. R. Assessing risk of neurodevelopmental disorders after birth with oxytocin: a systematic review and meta-analysis. *Psychological Medicine* **49,** 881–890 (2019).

11. Guastella, A. J. *et al.* Does perinatal exposure to exogenous oxytocin influence child behavioural problems and autistic-like behaviours to 20 years of age? *J.Child Psychol.Psychiatry* **2018/04/28,** (2018).

12. Soltys, S. M. *et al.* An association of intrapartum synthetic oxytocin dosing and the odds of developing autism. *Autism* **24,** 1400–1410 (2020).

13. Kenkel, W. *et al.* Behavioral and epigenetic consequences of oxytocin treatment at birth. *Science Advances* **5,** eaav2244 (2019).

14. Lawson, C. M., Rentrup, K. F. G., Cai, X., Kulkarni, P. P. & Ferris, C. F. Using multimodal MRI to investigate alterations in brain structure and function in the BBZDR/Wor rat model of type 2 diabetes. *Animal Models and Experimental Medicine* **3,** 285–294 (2020).

15. Kulkarni, P. *et al.* Characterizing the human APOE epsilon 4 knock-in transgene in female and male rats with multimodal magnetic resonance imaging. *Brain Research* **1747,** 147030 (2020).

16. Ferris, C. F. *et al.* Alterations in brain neurocircuitry following treatment with the chemotherapeutic agent paclitaxel in rats. *Neurobiology of Pain* **6,** 100034 (2019).

17. Yee, J. R. *et al.* BOLD fMRI in awake prairie voles: A platform for translational social and affective neuroscience. *Neuroimage* **138,** 221–232 (2016).

18. Ortiz, J. J., Portillo, W., Paredes, R. G., Young, L. J. & Alcauter, S. Resting state brain networks in the prairie vole. *Scientific Reports* **8,** (2018).

19. Ortiz, R. *et al.* Differences in Diffusion-Weighted Imaging and Resting-State Functional Connectivity Between Two Culturally Distinct Populations of Prairie Vole. *Biological Psychiatry: Cognitive Neuroscience and Neuroimaging* (2020). doi:10.1016/j.bpsc.2020.08.014

20. Worsley, K. J. in *Functional Magnetic Resonance Imaging* (Oxford University Press, 2001). doi:10.1093/acprof:oso/9780192630711.003.0014

21. Bastian, M., Heymann, S. & Jacomy, M. Gephi: An Open Source Software for Exploring and Manipulating Networks. *Proceedings of the International AAAI Conference on Web and Social Media* **3,** 361–362 (2009).

22. Worsley, K. J., Evans, A. C., Marrett, S. & Neelin, P. A Three-Dimensional Statistical Analysis for CBF Activation Studies in Human Brain. *J Cereb Blood Flow Metab* **12,** 900–918 (1992).

23. Freeman, L. C. A Set of Measures of Centrality Based on Betweenness. *Sociometry* **40,** 35–41 (1977).

24. Freeman, L. C. Centrality in social networks conceptual clarification. *Social Networks* **1,** 215–239 (1978).

25. Sabidussi, G. The centrality index of a graph. *Psychometrika* **31,** 581–603 (1966).

26. Carter, C. S. Developmental consequences of oxytocin. *Physiol Behav* **79,** 383–97 (2003).

27. Chiesa, M., Rabiei, H., Riffault, B., Ferrari, D. C. & Ben-Ari, Y. Brain Volumes in Mice are Smaller at Birth After Term or Preterm Cesarean Section Delivery. *Cereb Cortex* (2021). doi:10.1093/cercor/bhab033

28. Deoni, S. C. *et al.* PMC6330134; Cesarean Delivery Impacts Infant Brain Development. *AJNR Am.J.Neuroradiol.* **40,** 169–177 (2019).

Oxytocin Males

B **Oxytocin Females**

Control Females

Z score (|Z|)
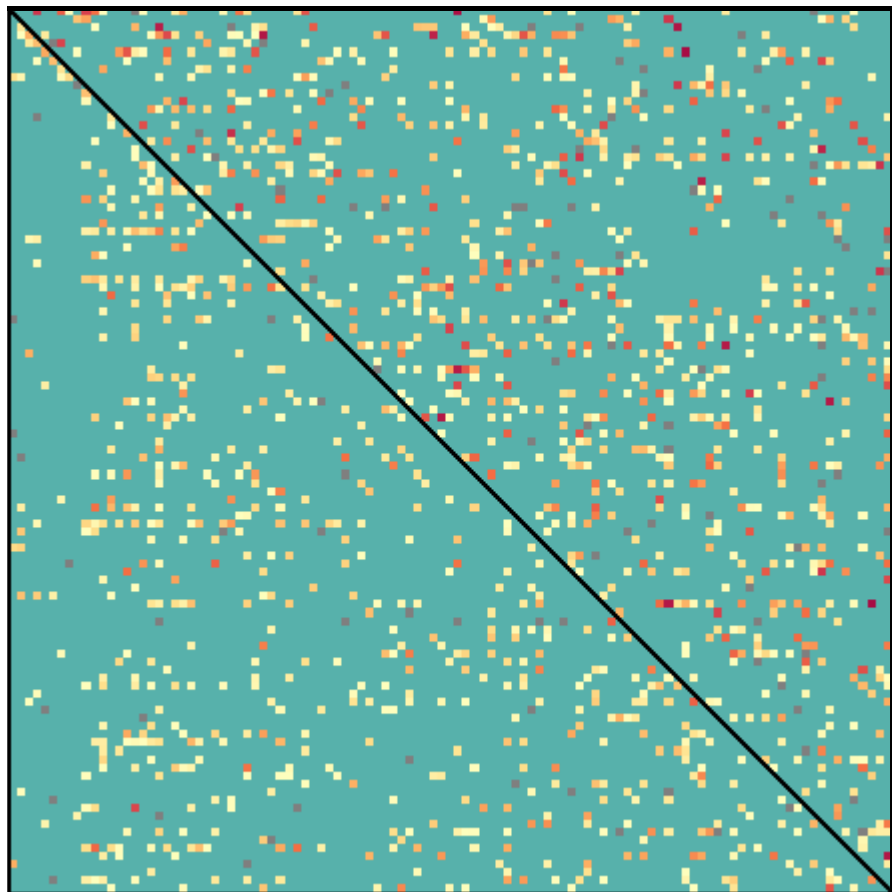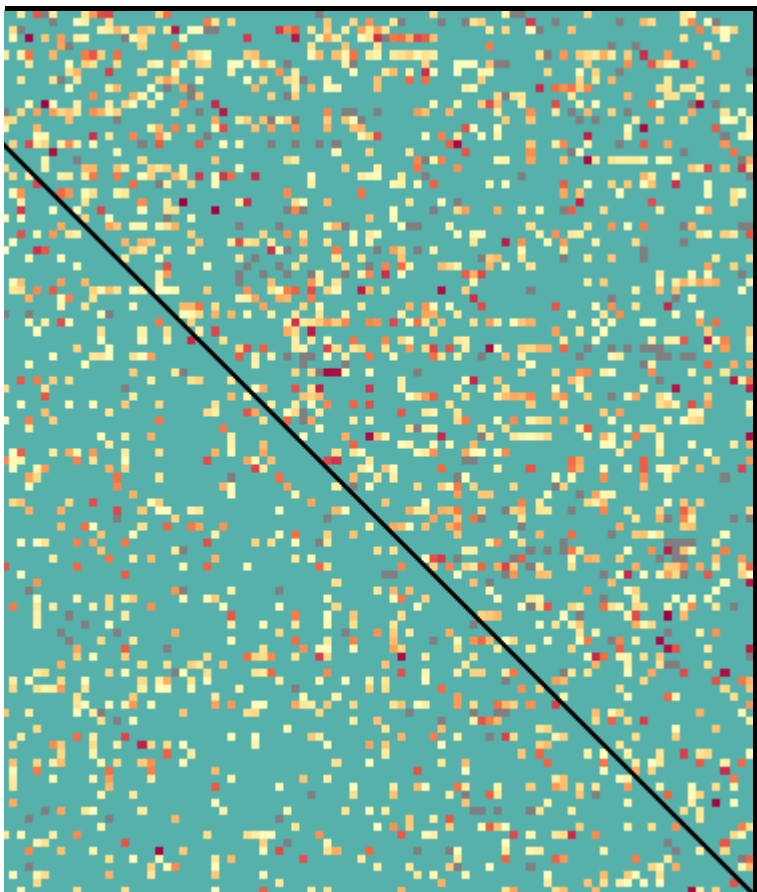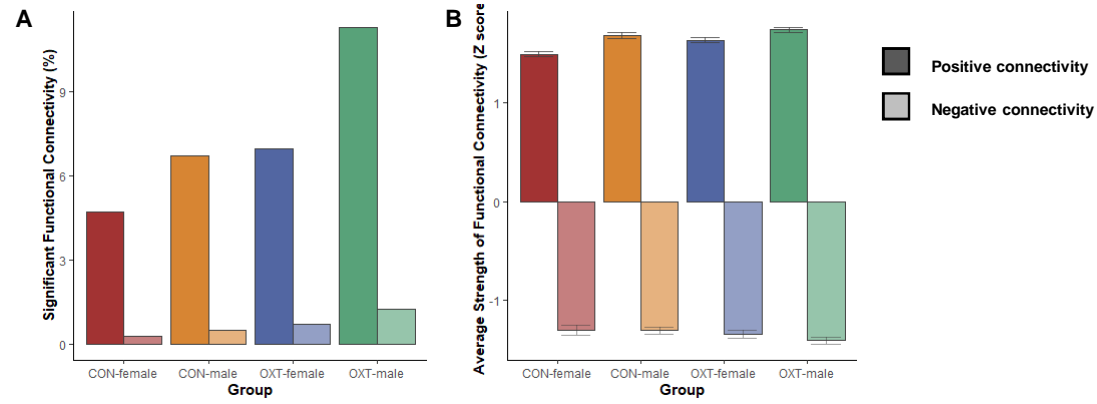
Figure X. (A) The proportion of all possible pairwise connections between brain regions that showed significant correlated activity (i.e. connectivity) in either a positive or negative direction for each group / sex. (B) The average strength, as expressed by z-score, of all significantly correlated connections in either a positive or negative direction for each group / sex.

Strength
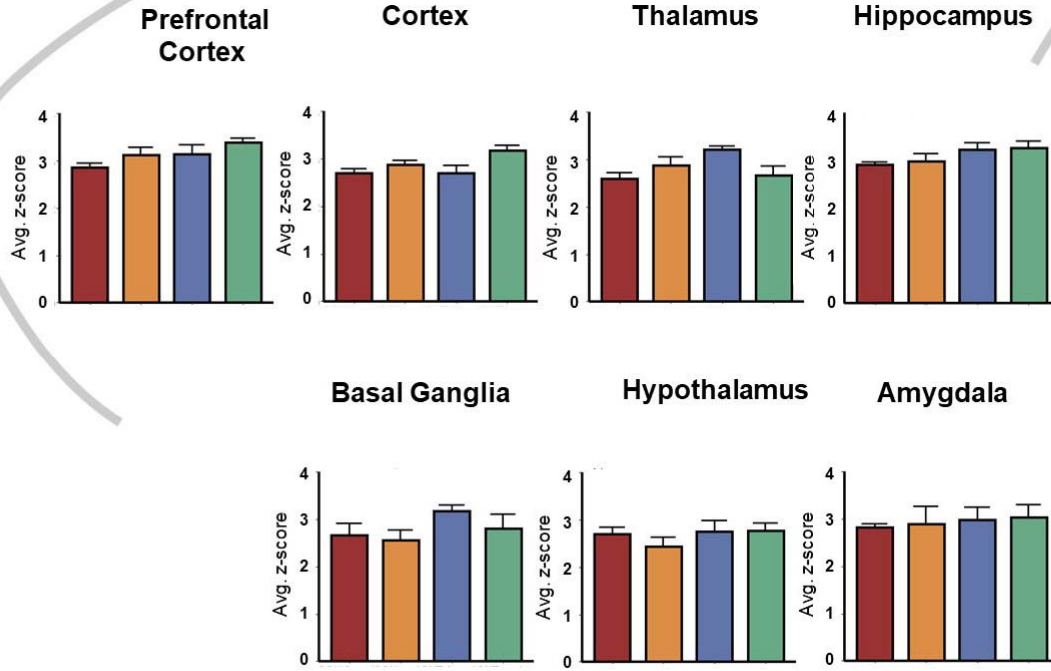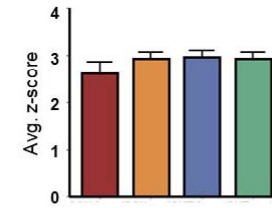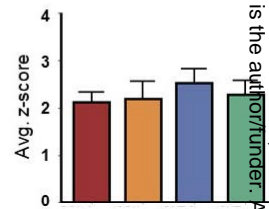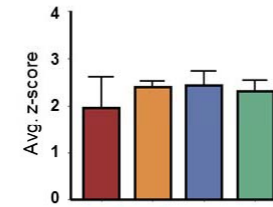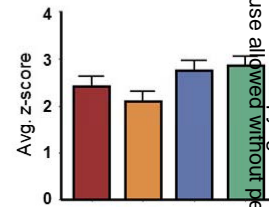
Betweenness
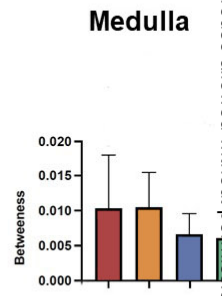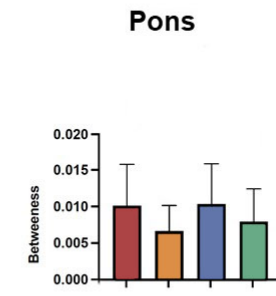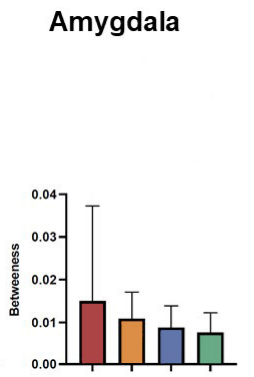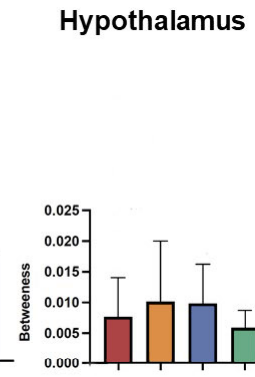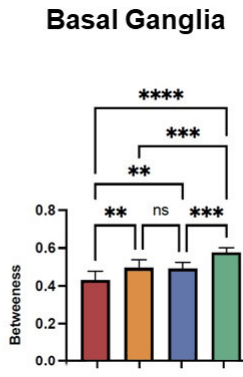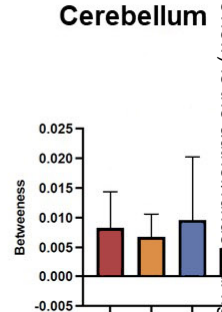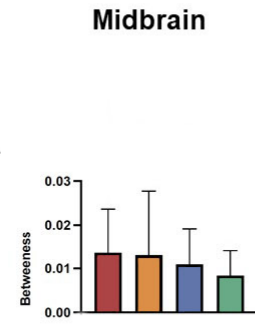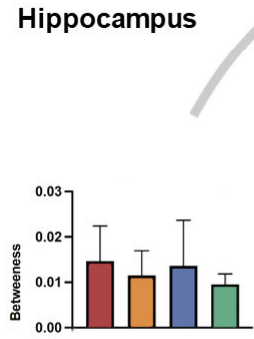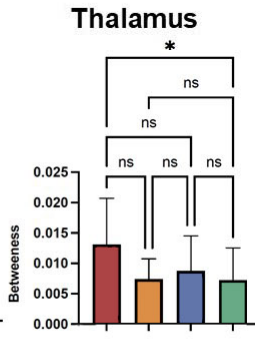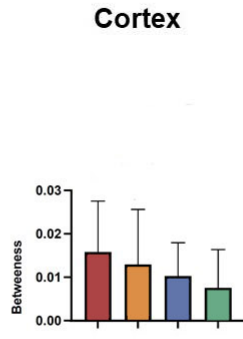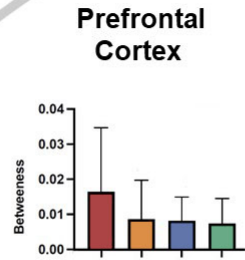
Closeness

CON female
CON male
OXT female
OXT male

Prefrontal Cortex

Cortex

Thalamus

Hippocampus

Olfactory System

Basal Ganglia

Hypothalamus

Amygdala

Midbrain

Cerebellum

Pons

Medulla
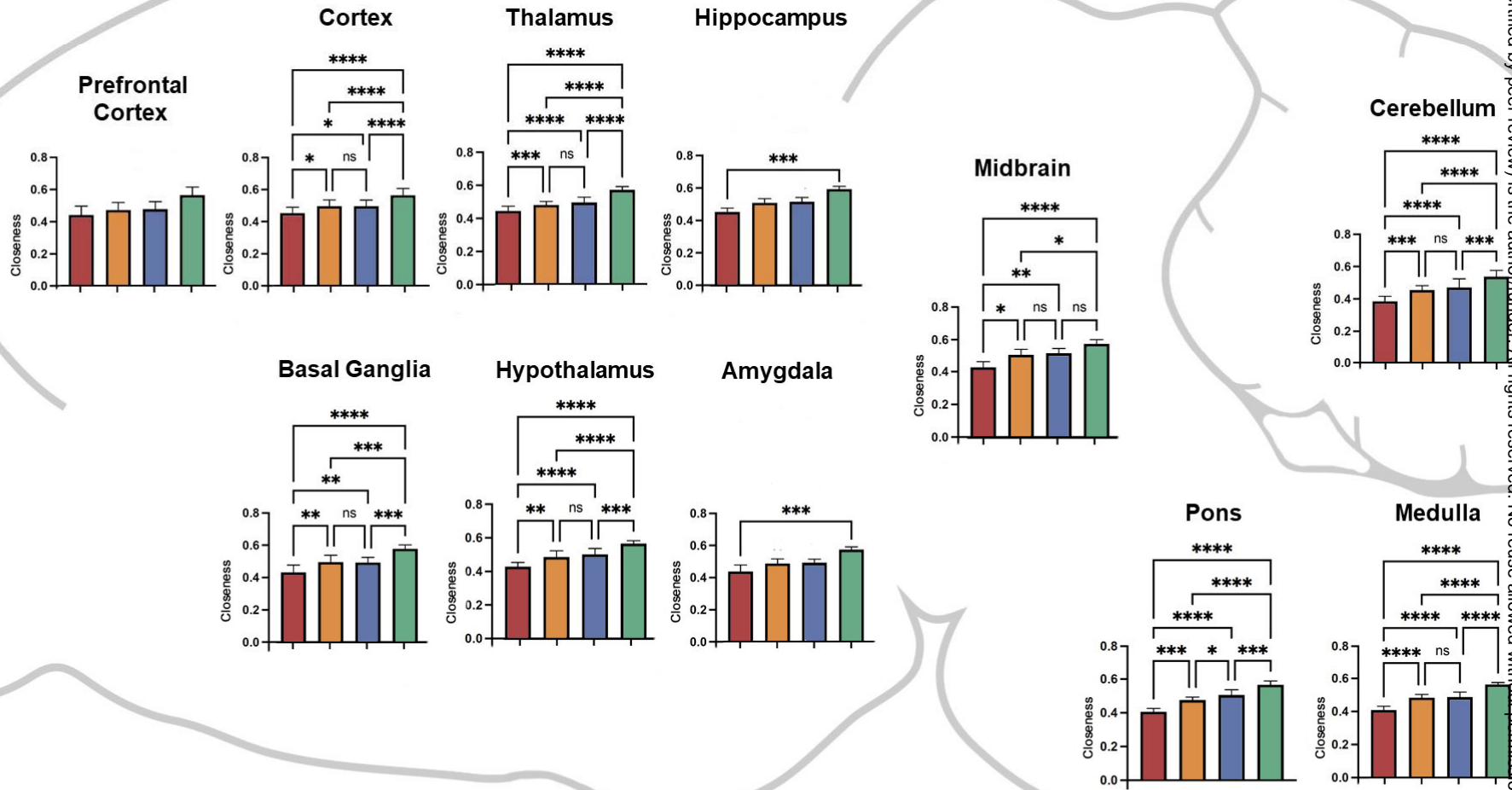
Degree

CON female

CON male

OXT female

OXT male

Olfactory System

Prefrontal Cortex

Cortex

Thalamus

Hippocampus

Basal Ganglia

Hypothalamus

Amygdala

Midbrain

Cerebellum

Pons

Medulla

FA PCA

B. **ADC PCA**

Dim1 (57%)

Dim2 (12.9%)

Dim1 (60.7%)

Groups
CON-female
CON-male
OXT-female
OXT-male

C.

ADC Dimension 1

group

CON-female CON-male OXT-female OXT-male
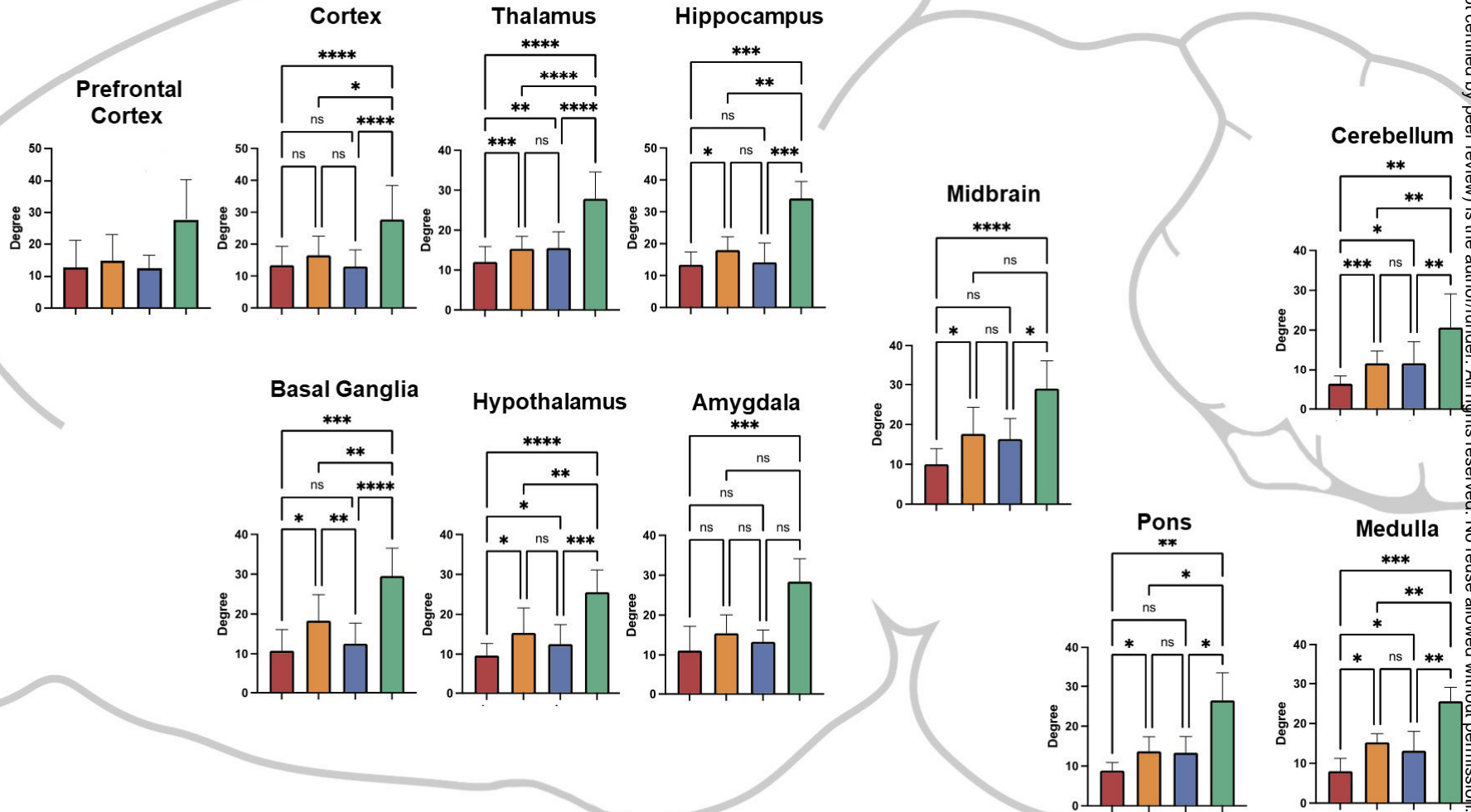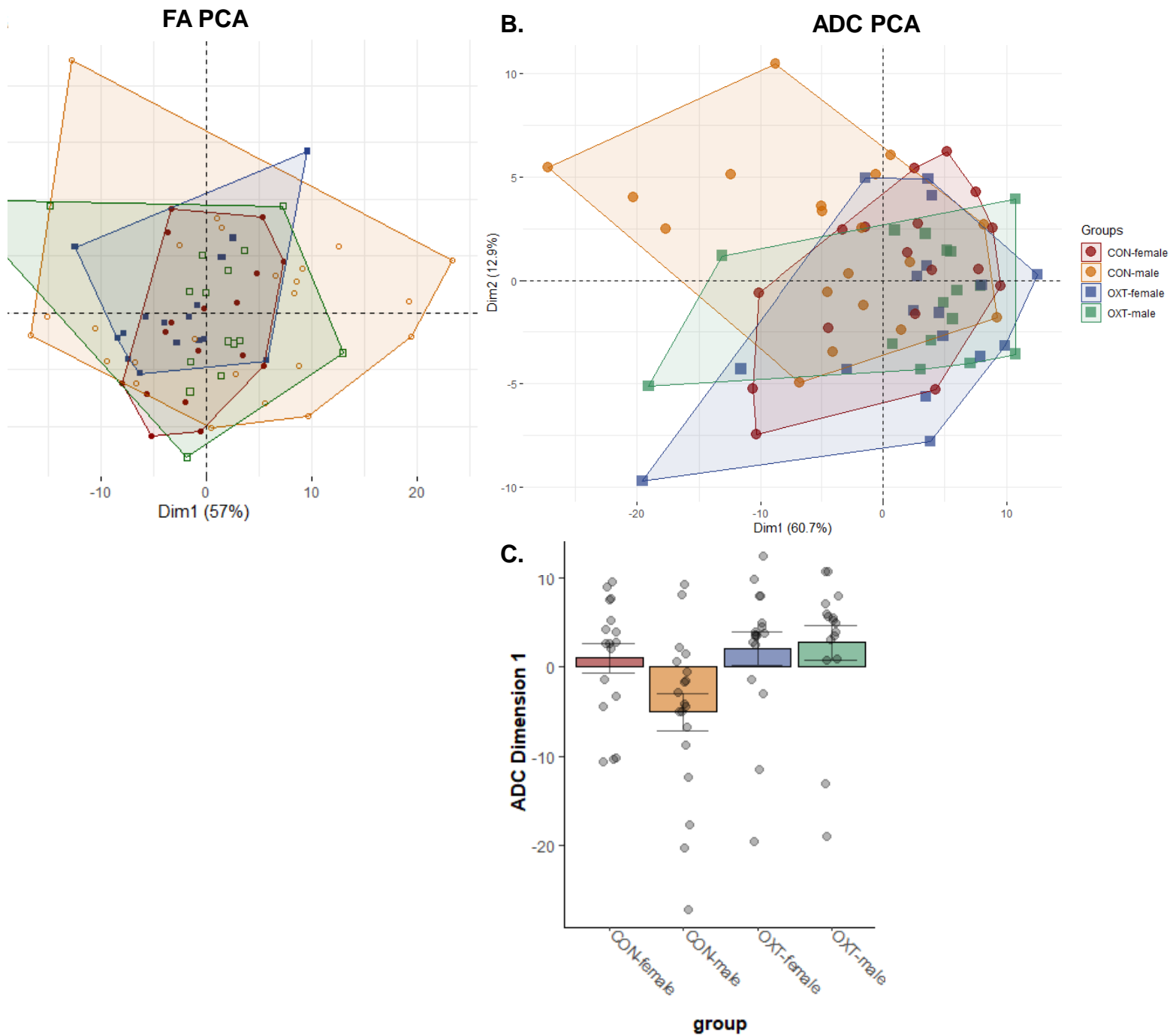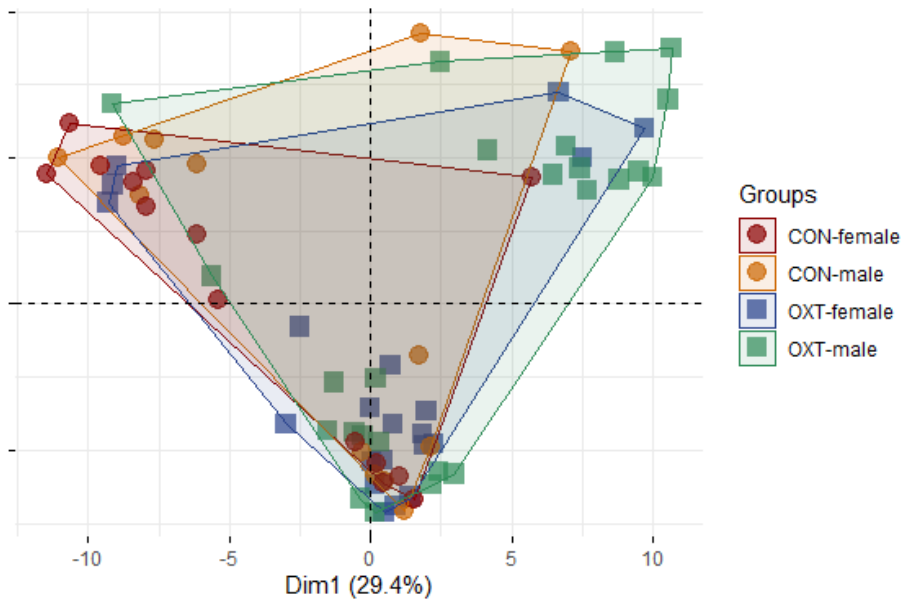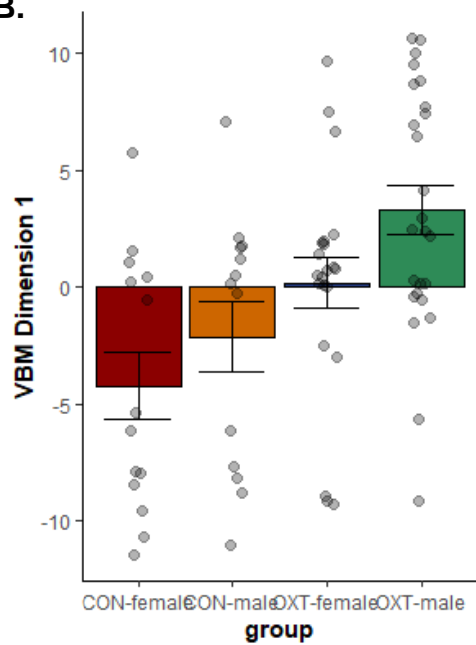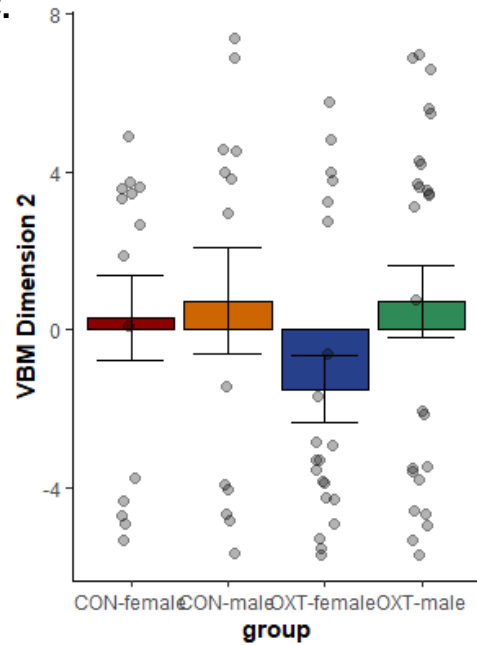
Apparent Diffusion Coefficient: Control Females and Males						
Brain Area	Females			Males		
	Mean	SD		Mean	SD	P val	Effect
cuneate nucleus	1.27	0.11	<	1.48	0.29	0.008	0.1919
9th cerebellar lobule	1.31	0.15	<	1.52	0.28	0.009	0.18698
tegmental nucleus	1.29	0.15	<	1.49	0.16	0.000	0.18492
7th cerebellar lobule	1.13	0.09	<	1.29	0.28	0.025	0.17274
parafascicular thalamic nucleus	1.24	0.11	<	1.41	0.18	0.001	0.17138
central medial thalamic nucleus	1.22	0.09	<	1.40	0.18	0.001	0.17085
dentate gyrus	1.40	0.15	<	1.60	0.22	0.003	0.17017
red nucleus	1.26	0.14	<	1.44	0.19	0.003	0.16745
perirhinal ctx	1.34	0.15	<	1.52	0.24	0.009	0.16346
habenula nucleus	1.34	0.11	<	1.52	0.24	0.009	0.15647
central amygdaloid nucleus	1.32	0.11	<	1.49	0.18	0.002	0.1552
ventral tegmental area	1.45	0.23	<	1.64	0.30	0.045	0.15392
reticular nucleus	1.29	0.09	<	1.46	0.18	0.002	0.15359
caudate putamen (striatum)	1.23	0.09	<	1.39	0.18	0.002	0.15305
accumbens core	1.25	0.10	<	1.40	0.15	0.001	0.14924
posterior thalamic nucleus	1.24	0.11	<	1.39	0.17	0.004	0.14636
globus pallidus	1.22	0.10	<	1.37	0.17	0.004	0.14432
zona incerta	1.32	0.16	<	1.47	0.21	0.018	0.14322
lateral amygdaloid nucleus	1.40	0.14	<	1.56	0.20	0.008	0.14169
temporal ctx	1.30	0.13	<	1.45	0.21	0.016	0.14155
median raphe nucleus	1.33	0.16	<	1.48	0.21	0.019	0.13934
parabrachial nucleus	1.31	0.14	<	1.46	0.17	0.008	0.13793
medial geniculate	1.26	0.12	<	1.40	0.17	0.007	0.13656
basal amygdaloid nucleus	1.31	0.17	<	1.45	0.18	0.021	0.13487
pontine reticular nucleus oral	1.34	0.21	<	1.48	0.22	0.047	0.13411
pretectal nucleus	1.28	0.10	<	1.42	0.18	0.007	0.13291
reticular formation	1.33	0.14	<	1.47	0.19	0.015	0.13201
claustrum	1.23	0.11	<	1.36	0.17	0.009	0.13179
White Matter	1.37	0.11	<	1.51	0.20	0.011	0.13133
reuniens nucleus	1.28	0.13	<	1.42	0.18	0.015	0.1309
ventral thalamic nuclei	1.28	0.11	<	1.41	0.18	0.010	0.13063
subiculum	1.40	0.16	<	1.55	0.20	0.021	0.12898
dorsal raphe	1.35	0.14	<	1.49	0.20	0.020	0.12782
lateral septal nucleus	1.45	0.12	<	1.60	0.18	0.008	0.12336
auditory ctx	1.29	0.12	<	1.42	0.19	0.023	0.12044
periaqueductal gray	1.41	0.11	<	1.55	0.22	0.027	0.11978
lateral posterior thalamic nucleus	1.30	0.10	<	1.43	0.17	0.012	0.11941
CA3	1.39	0.13	<	1.53	0.21	0.028	0.11874
posterior hypothalamic area	1.32	0.17	<	1.44	0.18	0.039	0.1185
infralimbic ctx	1.48	0.16	<	1.62	0.18	0.018	0.1179
CA1	1.40	0.12	<	1.53	0.19	0.017	0.11749

bed nucleus stria terminalis	1.30	0.13	<	1.43	0.17	0.019	0.11585
orbital ctx	1.36	0.14	<	1.48	0.21	0.046	0.11332
solitary tract nucleus	1.30	0.13	<	1.42	0.20	0.044	0.11314
paraventricular nuclus	1.37	0.15	<	1.49	0.16	0.022	0.11212
medial septum	1.34	0.14	<	1.46	0.14	0.022	0.10701
lateral geniculate	1.31	0.11	<	1.42	0.18	0.034	0.10652
extended amydala	1.33	0.15	<	1.44	0.17	0.043	0.10648

Fractional Anisotropy: Control Females and Males							
Brain Area	Females (n=17)			Males (n=19)			
	Mean	SD		Mean	SD	P val	Effect
parafascicular thalamic nucleus	0.48	0.06	>	0.39	0.07	0.000	0.32447
habenula nucleus	0.49	0.07	>	0.41	0.08	0.001	0.29116
lateral geniculate	0.56	0.05	>	0.47	0.07	0.000	0.26107
bed nucleus stria terminalis	0.48	0.04	>	0.41	0.05	0.000	0.26013
diagonal band of Broca	0.48	0.04	>	0.40	0.08	0.002	0.24076
claustrum	0.47	0.06	>	0.40	0.06	0.003	0.2303
lateral dorsal thalamic nucleus	0.58	0.05	>	0.51	0.10	0.005	0.21017
glomerular layer olfactory bulb	0.48	0.03	>	0.42	0.07	0.002	0.19975
lateral amygdaloid nucleus	0.50	0.08	>	0.43	0.08	0.020	0.19807
granular cell layer olfactory bulb	0.46	0.04	>	0.40	0.07	0.004	0.197
central medial thalamic nucleus	0.51	0.06	>	0.44	0.08	0.010	0.19131
pretectal nucleus	0.48	0.04	>	0.42	0.06	0.001	0.19005
ventral tegmental area	0.57	0.06	>	0.50	0.07	0.003	0.18642
anterior olfactory nucleus	0.48	0.03	>	0.42	0.06	0.001	0.1821
medial geniculate	0.52	0.04	>	0.46	0.08	0.005	0.18048
olfactory tubercles	0.52	0.03	>	0.46	0.07	0.002	0.17889
6th cerebellar lobule	0.48	0.05	>	0.42	0.06	0.003	0.178
medial preoptic area	0.51	0.03	>	0.45	0.08	0.006	0.17754
caudate putamen (striatum)	0.47	0.05	>	0.41	0.06	0.008	0.17608
posterior hypothalamic area	0.54	0.07	>	0.48	0.05	0.005	0.17523
orbital ctx	0.45	0.04	>	0.40	0.06	0.006	0.17508
tegmental nucleus	0.55	0.08	>	0.49	0.07	0.017	0.17139
reuniens nucleus	0.54	0.06	>	0.48	0.07	0.008	0.17084
dorsal raphe	0.52	0.07	>	0.46	0.08	0.024	0.17039
tenia tecta ctx	0.51	0.03	>	0.45	0.07	0.005	0.17023
red nucleus	0.53	0.06	>	0.47	0.07	0.010	0.16899
medial septum	0.48	0.07	>	0.43	0.07	0.035	0.16893
CA1	0.51	0.04	>	0.45	0.06	0.003	0.16838
posterior thalamic nucleus	0.52	0.03	>	0.46	0.07	0.004	0.16653
anterior thalamic nuclei	0.45	0.05	>	0.40	0.06	0.013	0.16469
substantia nigra	0.60	0.05	>	0.53	0.06	0.002	0.16259
secondary somaotsensory ctx	0.45	0.05	>	0.40	0.07	0.027	0.15839
lateral posterior thalamic nucleus	0.51	0.06	>	0.45	0.07	0.025	0.15525
CA3	0.53	0.04	>	0.47	0.07	0.007	0.15272
reticular formation	0.52	0.05	>	0.47	0.06	0.012	0.15052
dorsal medial nucleus	0.53	0.06	>	0.48	0.07	0.020	0.14557
accumbens core	0.53	0.04	>	0.48	0.06	0.003	0.14454
subiculum	0.49	0.04	>	0.45	0.06	0.011	0.13942
dentate gyrus	0.49	0.04	>	0.45	0.07	0.015	0.13789
ventral pallidum	0.53	0.04	>	0.48	0.06	0.008	0.13773
superior colliculus	0.44	0.04	>	0.40	0.06	0.019	0.13266

lateral preoptic area	0.56	0.04	>	0.51	0.08	0.023	0.1326
extended amydala	0.52	0.06	>	0.47	0.06	0.020	0.13195
parasubiculum	0.44	0.04	>	0.40	0.07	0.037	0.13104
median raphe nucleus	0.59	0.05	>	0.54	0.08	0.026	0.13094
interpeduncular nucleus	0.54	0.05	>	0.50	0.05	0.011	0.13013
7th cerebellar lobule	0.52	0.05	>	0.47	0.06	0.022	0.13013
accumbens shell	0.52	0.05	>	0.48	0.06	0.018	0.12372
zona incerta	0.64	0.05	>	0.58	0.07	0.018	0.11986
central amygdaloid nucleus	0.53	0.06	>	0.49	0.07	0.049	0.11951
8th cerebellar lobule	0.53	0.05	>	0.49	0.05	0.018	0.11938
endopiriform nucleus	0.49	0.06	>	0.45	0.05	0.046	0.11912
parabrachial nucleus	0.54	0.05	>	0.50	0.06	0.024	0.1173
paraventricular nuclus	0.55	0.06	>	0.50	0.07	0.040	0.11618
basal amygdaloid nucleus	0.56	0.05	>	0.51	0.07	0.046	0.11537
ventral thalamic nuclei	0.55	0.04	>	0.51	0.06	0.020	0.1152
9th cerebellar lobule	0.53	0.06	>	0.49	0.05	0.040	0.10817
pontine reticular nucleus oral	0.55	0.05	>	0.51	0.06	0.027	0.1075
cortical amygdaloid nucleus	0.53	0.04	>	0.50	0.06	0.040	0.10125
trigeminal complex medulla	0.53	0.02	>	0.49	0.05	0.007	0.09908
reticulotegmental nucleus	0.55	0.05	>	0.51	0.05	0.041	0.09501
crus ansiform lobule	0.50	0.04	>	0.47	0.05	0.040	0.08962

Fractional Anisotropy: Control Females vs Oxytocin Females						
Brain Area	Female Control		Female Oxytocin			
	Mean	SD	Mean	SD	P val	Effect
3rd cerebellar lobule	0.4825	0.0609	0.5259	0.0582	0.0235	0.11782
5th cerebellar lobule	0.489	0.0585	0.5273	0.0573	0.0388	0.10367
anterior cingulate ctx	0.478	0.0515	0.5141	0.0609	0.044	0.10039
inferior colliculus	0.4405	0.0436	0.4718	0.0561	0.0492	0.09499
auditory ctx	0.4565	0.0437	0.4886	0.0457	0.025	0.09415

Apparent Diffusion Coefficient: Control Males vs Oxytocin Males							
Brain Area	Males Control			Males Oxytocin			
	Mean	SD		Mean	SD	P val	Effect
periaqueductal gray	1.55	0.22	>	1.31	0.14	0.000	0.25266
tegmental nucleus	1.49	0.16	>	1.26	0.13	0.000	0.24327
vestibular nucleus	1.48	0.16	>	1.26	0.15	0.000	0.22849
dorsal raphe	1.49	0.20	>	1.28	0.14	0.000	0.22449
Ventricle	1.79	0.22	>	1.62	0.11	0.000	0.14191
parafascicular thalamic nucleus	1.41	0.18	>	1.22	0.12	0.000	0.22109
reuniens nucleus	1.42	0.18	>	1.22	0.14	0.000	0.22122
paraventricular nuclus	1.49	0.16	>	1.29	0.13	0.000	0.21074
posterior thalamic nucleus	1.39	0.17	>	1.21	0.13	0.000	0.20552
superior colliculus	1.45	0.19	>	1.26	0.13	0.000	0.20326
ventral thalamic nuclei	1.41	0.18	>	1.23	0.14	0.000	0.19862
CA3	1.53	0.21	>	1.33	0.15	0.000	0.20163
central amygdaloid nucleus	1.49	0.18	>	1.31	0.14	0.000	0.19427
central medial thalamic nucleus	1.40	0.18	>	1.22	0.12	0.000	0.19809
lateral amygdaloid nucleus	1.56	0.20	>	1.39	0.13	0.000	0.17413
medial dorsal thalamic nucleus	1.40	0.19	>	1.22	0.14	0.000	0.20071
pretectal nucleus	1.42	0.18	>	1.25	0.12	0.000	0.18295
secondary somaotsensory ctx	1.42	0.17	>	1.27	0.13	0.000	0.16995
medial geniculate	1.40	0.17	>	1.24	0.14	0.000	0.18186
bed nucleus stria terminalis	1.43	0.17	>	1.26	0.13	0.000	0.18427
accumbens core	1.40	0.15	>	1.24	0.12	0.000	0.17873
CA1	1.53	0.19	>	1.36	0.15	0.000	0.17772
lateral dorsal thalamic nucleus	1.48	0.18	>	1.32	0.13	0.000	0.16654
parabrachial nucleus	1.46	0.17	>	1.30	0.16	0.000	0.16313
lateral posterior thalamic nucleus	1.43	0.17	>	1.26	0.14	0.000	0.17875
red nucleus	1.44	0.19	>	1.27	0.14	0.000	0.18789
primary somatosensory ctx	1.55	0.21	>	1.39	0.17	0.001	0.15046
reticular nucleus	1.46	0.18	>	1.29	0.13	0.001	0.17881
inferior colliculus	1.50	0.21	>	1.30	0.14	0.001	0.20488
habenula nucleus	1.52	0.24	>	1.35	0.19	0.001	0.16646
medial septum	1.46	0.14	>	1.29	0.13	0.001	0.17305
paraventricular nucleus	1.40	0.19	>	1.23	0.17	0.001	0.18977
White Matter	1.51	0.20	>	1.35	0.15	0.001	0.16027
lateral geniculate	1.42	0.18	>	1.25	0.13	0.001	0.17768
2nd cerebellar lobule	1.47	0.20	>	1.30	0.21	0.001	0.17439
caudate putamen (striatum)	1.39	0.18	>	1.23	0.12	0.001	0.16938
claustrum	1.36	0.17	>	1.21	0.11	0.001	0.16714
anterior thalamic nuclei	1.40	0.18	>	1.24	0.15	0.001	0.17436
median raphe nucleus	1.48	0.21	>	1.33	0.17	0.001	0.14888
reticular formation	1.47	0.19	>	1.31	0.19	0.001	0.16269
accumbens shell	1.43	0.16	>	1.26	0.14	0.002	0.18139

auditory ctx	1.42	0.19	>	1.27	0.16	0.002	0.1609
globus pallidus	1.37	0.17	>	1.21	0.14	0.002	0.17193
orbital ctx	1.48	0.21	>	1.31	0.14	0.003	0.17342
infralimbic ctx	1.62	0.18	>	1.44	0.16	0.003	0.16252
7th cerebellar lobule	1.29	0.28	>	1.08	0.18	0.003	0.26364
visual 1 ctx	1.50	0.25	>	1.34	0.19	0.003	0.15891
anterior olfactory nucleus	1.57	0.30	>	1.35	0.22	0.003	0.21393
10th cerebellar lobule	1.62	0.25	>	1.43	0.17	0.003	0.18096
dentate gyrus	1.60	0.22	>	1.41	0.19	0.003	0.18057
agranular insular ctx	1.45	0.17	>	1.30	0.23	0.004	0.1574
5th cerebellar lobule	1.25	0.24	>	1.07	0.19	0.004	0.22931
extended amydala	1.44	0.17	>	1.29	0.17	0.004	0.15247
3rd cerebellar lobule	1.30	0.22	>	1.13	0.21	0.004	0.20307
endopiriform nucleus	1.40	0.18	>	1.26	0.18	0.005	0.15393
6th cerebellar lobule	1.24	0.23	>	1.03	0.18	0.005	0.26201
parasubiculum	1.57	0.28	>	1.42	0.21	0.005	0.14979
subiculum	1.55	0.20	>	1.40	0.24	0.007	0.13718
frontal association ctx	1.58	0.24	>	1.43	0.19	0.008	0.15083
zona incerta	1.47	0.21	>	1.31	0.22	0.011	0.17364
temporal ctx	1.45	0.21	>	1.30	0.22	0.012	0.15813
lateral septal nucleus	1.60	0.18	>	1.48	0.12	0.012	0.10938
primary motor ctx	1.60	0.27	>	1.49	0.19	0.014	0.09447
visual 2 ctx	1.66	0.31	>	1.52	0.20	0.015	0.12248
ventral pallidum	1.47	0.18	>	1.32	0.18	0.015	0.15104
pontine reticular nucleus oral	1.48	0.22	>	1.36	0.27	0.016	0.12224
solitary tract nucleus	1.42	0.20	>	1.28	0.21	0.016	0.14862
retrosplenial ctx	1.77	0.33	>	1.64	0.22	0.016	0.10686
basal amygdaloid nucleus	1.45	0.18	>	1.30	0.23	0.022	0.16251
anterior hypothalamic area	1.55	0.23	>	1.39	0.27	0.023	0.1591
9th cerebellar lobule	1.52	0.28	>	1.33	0.19	0.024	0.18827
posterior hypothalamic area	1.44	0.18	>	1.28	0.16	0.024	0.17083
medial preoptic area	1.57	0.25	>	1.41	0.23	0.024	0.15719
diagonal band of Broca	1.53	0.22	>	1.40	0.21	0.025	0.13414
pontine reticular nucleus caudal	1.49	0.22	>	1.38	0.34	0.025	0.1033
perirhinal ctx	1.52	0.24	>	1.36	0.31	0.028	0.16618
anterior cingulate ctx	1.75	0.24	>	1.58	0.20	0.028	0.14404
crus ansiform lobule	1.36	0.24	>	1.23	0.23	0.029	0.1512
8th cerebellar lobule	1.38	0.29	>	1.23	0.24	0.034	0.1625
gigantocellular reticular nucleus	1.53	0.26	>	1.43	0.38	0.036	0.10108
granular cell layer olfactory bulb	1.56	0.30	>	1.40	0.16	0.040	0.16061
cuneate nucleus	1.48	0.29	>	1.34	0.25	0.042	0.14091
dorsal medial nucleus	1.64	0.25	>	1.51	0.20	0.046	0.11454
medial amygdaloid nucleus	1.68	0.25	>	1.52	0.34	0.049	0.13551

Fractional Anisotropy: Control Males vs Oxytocin Males						
Brain Area	Males Control			Males Oxytocin		
	Mean	SD		Mean	SD	P val	Effect
medial preoptic area	0.47	0.06	<	0.52	0.06	0.004	0.1249
pontine nuclei	0.50	0.07	<	0.53	0.04	0.001	0.09148
medial geniculate	0.55	0.06	<	0.59	0.05	0.024	0.07966
median raphe nucleus	0.52	0.05	<	0.56	0.06	0.015	0.07972
lateral geniculate	0.52	0.06	<	0.56	0.05	0.009	0.08229
parabrachial nucleus	0.51	0.03	<	0.53	0.05	0.012	0.05862
lateral dorsal thalamic nucleus	0.50	0.06	<	0.53	0.05	0.005	0.079
reticular formation	0.52	0.05	<	0.54	0.05	0.002	0.0676
lemniscal nucleus	0.55	0.03	<	0.57	0.04	0.002	0.04745
anterior olfactory nucleus	0.48	0.07	<	0.51	0.03	0.023	0.07136
3rd cerebellar lobule	0.51	0.04	<	0.53	0.04	0.001	0.04758
ventral pallidum	0.46	0.04	<	0.49	0.06	0.026	0.07166
ventral medial nucleus	0.56	0.05	>	0.53	0.05	0.015	0.06245
reuniens nucleus	0.48	0.05	<	0.51	0.05	0.043	0.06446
trigeminal complex pons	0.51	0.06	<	0.53	0.06	0.007	0.06633
agranular insular ctx	0.55	0.06	<	0.57	0.04	0.014	0.05201
cortical amygdaloid nucleus	0.52	0.06	<	0.54	0.05	0.037	0.05807
auditory ctx	0.49	0.04	<	0.51	0.04	0.049	0.04631
medial amygdaloid nucleus	0.47	0.06	>	0.44	0.08	0.032	0.08558
periaqueductal gray	0.51	0.06	<	0.53	0.06	0.023	0.05655
ventral thalamic nuclei	0.50	0.05	<	0.53	0.07	0.027	0.05859
2nd cerebellar lobule	0.47	0.05	<	0.50	0.08	0.005	0.06362
posterior thalamic nucleus	0.52	0.06	<	0.54	0.04	0.006	0.04344
paraventricular nucleus, hypothalamus	0.48	0.06	<	0.50	0.07	0.009	0.05594
superior colliculus	0.45	0.04	<	0.46	0.06	0.012	0.05009
reticulotegmental nucleus	0.53	0.05	<	0.54	0.04	0.009	0.03172
frontal association ctx	0.53	0.05	<	0.55	0.05	0.049	0.0364
prelimbic ctx	0.53	0.05	<	0.54	0.04	0.047	0.02827
olivary nucleus	0.48	0.06	<	0.50	0.05	0.036	0.04071
central medial thalamic nucleus	0.52	0.05	<	0.54	0.06	0.017	0.0384
Ventricle	0.52	0.06	<	0.54	0.06	0.029	0.04214
reticular nucleus	0.48	0.07	<	0.50	0.05	0.033	0.04473
lateral preoptic area	0.52	0.05	<	0.53	0.04	0.001	0.03037
tegmental nucleus	0.50	0.05	<	0.52	0.07	0.011	0.03654
CA3	0.49	0.04	<	0.50	0.04	0.024	0.02462
lateral amygdaloid nucleus	0.50	0.04	<	0.51	0.07	0.028	0.03662
nucleus lateral olfactory tract	0.46	0.04	<	0.47	0.06	0.047	0.02991
medial dorsal thalamic nucleus	0.48	0.04	<	0.48	0.06	0.040	0.0247
subiculum	0.53	0.05	<	0.54	0.04	0.014	0.01905
8th cerebellar lobule	0.49	0.05	<	0.50	0.06	0.029	0.02393
CA1	0.48	0.03	<	0.49	0.06	0.042	0.0192
lateral septal nucleus	0.52	0.08	<	0.53	0.07	0.011	0.02664
accumbens shell	0.51	0.06	<	0.52	0.06	0.012	0.02132

entorhinal ctx	0.45	0.05	<	0.46	0.07	0.017	0.02447
paraflocculus cerebellum	0.50	0.03	>	0.49	0.07	0.047	0.01945
extended amydala	0.53	0.05	<	0.54	0.04	0.003	0.01581
inferior colliculus	0.47	0.04	<	0.47	0.07	0.008	0.02053
endopiriform nucleus	0.44	0.05	<	0.44	0.07	0.041	0.02301
visual 2 ctx	0.53	0.08	<	0.54	0.06	0.045	0.01821
substantia nigra	0.52	0.06	<	0.52	0.05	0.010	0.01221
central amygdaloid nucleus	0.45	0.04	<	0.45	0.06	0.037	0.01297
olfactory tubercles	0.49	0.08	<	0.50	0.07	0.034	0.01172
retrosplenial ctx	0.50	0.03	>	0.50	0.06	0.024	0.00761
7th cerebellar lobule	0.49	0.06	<	0.50	0.06	0.046	0.00868
lateral hypothalamus	0.45	0.05	<	0.45	0.07	0.033	0.00705
diagonal band of Broca	0.50	0.04	<	0.50	0.05	0.007	0.00393
mammillary nucleus	0.46	0.05	<	0.46	0.07	0.028	0.00318

Apparent Diffusion Coefficient: Oxytocin Females and Males							
Brain Area	Females			Males			
	Mean	SD		Mean	SD	P val	Effect
posterior hypothalamic area	1.36	0.20	>	1.28	0.16	0.204	0.08826
lateral amygdaloid nucleus	1.33	0.14	<	1.39	0.13	0.210	0.06107
paraventricular nuclus	1.36	0.17	>	1.29	0.13	0.214	0.07412
periaqueductal gray	1.37	0.15	>	1.31	0.14	0.215	0.06965
olfactory tubercles	1.81	0.45	>	1.64	0.39	0.245	0.14519
lateral paragigantocellular nucleus	2.06	0.58	>	1.85	0.44	0.248	0.15664
lateral septal nucleus	1.43	0.13	<	1.48	0.12	0.279	0.04608
anterior hypothalamic area	1.51	0.35	>	1.39	0.27	0.295	0.1161
tegmental nucleus	1.31	0.14	>	1.26	0.13	0.316	0.05427
tenia tecta ctx	1.59	0.30	>	1.50	0.25	0.355	0.0843
Ventricle	1.58	0.15	<	1.62	0.11	0.367	0.03688
medial preoptic area	1.48	0.28	>	1.41	0.23	0.415	0.07321
secondary somaotsensory ctx	1.23	0.13	<	1.27	0.13	0.439	0.04088
diagonal band of Broca	1.46	0.25	>	1.40	0.21	0.443	0.06346
lateral preoptic area	1.49	0.29	>	1.41	0.24	0.448	0.07056
dorsal raphe	1.32	0.12	>	1.28	0.14	0.456	0.03791
reuniens nucleus	1.26	0.16	>	1.22	0.14	0.465	0.04513
6th cerebellar lobule	1.08	0.16	>	1.03	0.18	0.469	0.06025
prelimbic ctx	1.45	0.15	<	1.49	0.15	0.472	0.03677
perirhinal ctx	1.28	0.27	<	1.36	0.31	0.480	0.07554
pontine reticular nucleus oral	1.42	0.22	>	1.36	0.27	0.488	0.06303
caudate putamen (striatum)	1.21	0.12	<	1.23	0.12	0.524	0.03158
habenula nucleus	1.31	0.15	<	1.35	0.19	0.526	0.04112
medial amygdaloid nucleus	1.60	0.35	>	1.52	0.34	0.528	0.07104
trigeminal complex pons	1.81	0.44	>	1.71	0.43	0.531	0.07762
anterior amygdaloid nucleus	1.62	0.33	>	1.54	0.41	0.533	0.07465
auditory ctx	1.24	0.10	<	1.27	0.16	0.533	0.03382
dorsal medial nucleus	1.59	0.48	>	1.51	0.20	0.534	0.07237
2nd cerebellar lobule	1.34	0.20	>	1.30	0.21	0.538	0.04769
claustrum	1.18	0.14	<	1.21	0.11	0.539	0.03185
primary motor ctx	1.46	0.17	<	1.49	0.19	0.556	0.03508
medullary reticular nucleus	1.89	0.64	>	1.78	0.46	0.578	0.08247
paraflocculus cerebellum	1.63	0.59	>	1.53	0.41	0.579	0.0861
CA1	1.39	0.17	>	1.36	0.15	0.580	0.03361
raphe magnus	2.01	0.68	>	1.89	0.55	0.580	0.08568
ventral thalamic nuclei	1.26	0.14	>	1.23	0.14	0.585	0.03056
vestibular nucleus	1.29	0.12	>	1.26	0.15	0.586	0.02905
temporal ctx	1.26	0.18	<	1.30	0.22	0.587	0.04304
gigantocellular reticular nucleus	1.50	0.37	>	1.43	0.38	0.600	0.06719
superior colliculus	1.29	0.15	>	1.26	0.13	0.605	0.02826
retrosplenial ctx	1.60	0.20	<	1.64	0.22	0.605	0.03314

zona incerta	1.35	0.23	>	1.31	0.22	0.606	0.04358
9th cerebellar lobule	1.31	0.13	<	1.33	0.19	0.615	0.03052
nucleus lateral olfactory tract	1.79	0.59	>	1.68	0.67	0.622	0.08873
subiculum	1.46	0.35	>	1.40	0.24	0.625	0.05103
lateral hypothalamus	1.69	0.42	>	1.62	0.35	0.638	0.05419
cuneate nucleus	1.31	0.16	<	1.34	0.25	0.645	0.0363
reticular formation	1.34	0.19	>	1.31	0.19	0.663	0.03163

Fractional Anisotropy: Oxytocin Females and Males							
Brain Area	Females (n=17)			Males (n=16)			
	Mean	SD		Mean	SD	P val	Effect
posterior hypothalamic area	0.55	0.07	>	0.50	0.09	0.075	0.14445
parafascicular thalamic nucleus	0.48	0.07	>	0.44	0.09	0.197	0.12223
ventral tegmental area	0.56	0.06	>	0.52	0.06	0.064	0.1192
habenula nucleus	0.48	0.09	>	0.45	0.09	0.253	0.11422
bed nucleus stria terminalis	0.50	0.06	>	0.46	0.09	0.191	0.11089
parietal ctx	0.49	0.05	>	0.46	0.08	0.181	0.10247
dorsal medial nucleus	0.55	0.08	>	0.51	0.08	0.234	0.09392
10th cerebellar lobule	0.53	0.04	>	0.49	0.05	0.073	0.09293
nucleus lateral olfactory tract	0.51	0.07	>	0.48	0.06	0.218	0.08411
dentate gyrus	0.52	0.04	>	0.49	0.08	0.235	0.0829
ventral medial nucleus	0.51	0.07	<	0.54	0.04	0.141	0.08217
diagonal band of Broca	0.45	0.06	>	0.48	0.10	0.355	0.08207
lateral amygdaloid nucleus	0.51	0.05	>	0.49	0.09	0.301	0.08167
CA3	0.54	0.04	>	0.51	0.07	0.181	0.08134
claustrum	0.47	0.06	>	0.44	0.10	0.371	0.0808
secondary motor ctx	0.48	0.06	>	0.45	0.09	0.373	0.08001
interpeduncular nucleus	0.54	0.06	>	0.51	0.06	0.228	0.07444
substantia nigra	0.59	0.04	>	0.56	0.05	0.121	0.06825
primary motor ctx	0.47	0.05	>	0.45	0.09	0.442	0.06572
pontine nuclei	0.49	0.10	>	0.51	0.03	0.356	0.06518
9th cerebellar lobule	0.54	0.05	>	0.51	0.05	0.202	0.06355
parvicellular reticular nucleus	0.53	0.05	>	0.51	0.06	0.271	0.05979
anterior olfactory nucleus	0.49	0.03	>	0.47	0.07	0.351	0.05818
tenia tecta ctx	0.52	0.04	>	0.50	0.07	0.349	0.05668
facial nucleus medulla	0.52	0.04	>	0.50	0.05	0.245	0.05523
primary somatosensory ctx	0.47	0.05	>	0.45	0.08	0.481	0.05419
lateral geniculate	0.55	0.04	>	0.53	0.06	0.302	0.05357
lemniscal nucleus	0.52	0.05	>	0.54	0.04	0.198	0.05312
red nucleus	0.54	0.06	>	0.52	0.09	0.488	0.05294
medial geniculate	0.53	0.05	>	0.52	0.08	0.419	0.05289
ventral thalamic nuclei	0.57	0.05	>	0.55	0.06	0.323	0.05265
medullary reticular nucleus	0.55	0.06	>	0.53	0.05	0.306	0.05185
olfactory tubercles	0.52	0.04	>	0.50	0.06	0.340	0.0492
8th cerebellar lobule	0.54	0.05	>	0.53	0.05	0.274	0.04893
infralimbic ctx	0.51	0.05	>	0.53	0.07	0.393	0.04893
lateral preoptic area	0.57	0.06	>	0.55	0.07	0.437	0.04858
central medial thalamic nucleus	0.52	0.07	>	0.50	0.08	0.527	0.04685
visual 2 ctx	0.51	0.05	>	0.50	0.07	0.458	0.0467
prelimbic ctx	0.46	0.06	>	0.45	0.08	0.575	0.04665
orbital ctx	0.46	0.04	>	0.45	0.08	0.523	0.04541
visual 1 ctx	0.50	0.05	>	0.48	0.06	0.447	0.0454

cuneate nucleus	0.53	0.05	>	0.52	0.05	0.348	*0.04477*
reuniens nucleus	0.55	0.07	>	0.53	0.08	0.520	*0.04428*
Pon	0.51	0.07	>	0.52	0.04	0.419	*0.04358*
posterior thalamic nucleus	0.54	0.05	>	0.52	0.08	0.508	*0.04352*
vestibular nucleus	0.51	0.05	>	0.50	0.06	0.460	*0.04265*
granular cell layer olfactory bulb	0.47	0.04	>	0.45	0.07	0.513	*0.04214*
6th cerebellar lobule	0.51	0.07	>	0.50	0.06	0.516	*0.04205*